

Plasmachemical Amine Functionalization of Porous Polystyrene Beads: The Importance of Pore Architecture

G. Øye, V. Roucoules, A. M. Cameron, L. J. Oates, N. R. Cameron,
P. G. Steel, and J. P. S. Badyal*

*Department of Chemistry, Science Laboratories, Durham University,
Durham DH1 3LE, England, United Kingdom*

B. G. Davis

*Dyson Perrins Laboratory, Department of Chemistry, University of Oxford,
Oxford OX1 3QY, England, United Kingdom*

D. Coe and R. Cox

*GlaxoSmithKline, Medicines Research Centre, Gunnels Wood Road,
Stevenage SG1 2NY, England, United Kingdom*

Received March 27, 2002. In Final Form: June 21, 2002

The functionalization of different types of porous polystyrene microspheres using allylamine plasmas has been explored using a combination of Fmoc derivatization chemistry and cross-sectional Raman microscopy. Higher amine group loadings are obtained for small particles with large internal pore diameters.

1. Introduction

Functionalized porous polymer beads are widely employed for solid-phase organic synthesis,^{1,2} combinatorial chemistry,³ polymer-supported catalysis,^{4,5} and ion-exchange resins.^{6,7} Typically, the desired functionality is incorporated into the porous polymer bead structure by functional monomer copolymerization.⁸ However, the number of commercially available monomers for this purpose is fairly limited, which in turn restricts the types of surface functionality. Alternative approaches employed in the past to circumvent this problem have included grafting⁹ and plasmachemical functionalization.¹⁰ The latter is particularly appealing since it can be easily applied to a wide variety of solid supports and is regarded as being comparatively quick, cheap, and solventless.¹¹ Despite there being several previous studies related to the plasma modification of porous polymer beads to give, for example, fluorocarbon¹² and amine^{10,13} groups, there currently exists very little understanding concerning the

roles played by bead morphology and pore architecture (e.g., surface area, particle size, pore size distribution, etc.).

In this article, we investigate how the level of plasma-chemical amine functionalization of porous polymer microspheres depends on particle diameter and internal pore size distribution. Allylamine (CH₂=CH-CH₂-NH₂) has been chosen as the precursor molecule for plasma polymerization, since it contains a carbon-carbon double bond susceptible to polymerization via electrical discharge activation and also a primary amine group suited for application in solid-phase organic synthesis. A combination of N₂ sorption measurements, Fmoc derivatization of amine groups, scanning electron microscopy (SEM) analysis, and Raman microscopy has been employed to determine the level and spatial proximity of plasmachemical functionalization in the treated beads.

2. Experimental Section

A range of commercially available porous polystyrene beads were employed in this study: ArgoPore (Argonaut Technologies), PM3-0001 (Biosearch Technologies), Amberchrom CG-1000 (TosoHaas), Dynospheres PD-30 (DynaL Particles), and Dynospheres PD-15 (DynaL Particles), Table 1.

Nitrogen sorption analysis of the polystyrene beads was performed at 77 K (Micromeritics, TriStar 3000 surface area and porosimetry analyzer). Each sample was degassed at 50 °C for 12 h prior to characterization. The specific surface area and the pore volume values were estimated according to the Brunauer-Emmett-Teller (BET) and Barrett-Joyner-Halenda (BJH) models, respectively.^{14–16}

Plasma polymerization experiments were carried out in a rotating glass reactor pumped continuously by a two-stage rotary

* To whom correspondence should be addressed.

(1) Rana, S.; Dubuc, J.; Bradley, M.; White, P. *Tetrahedron Lett.* **2000**, *41*, 5135.

(2) Fruchtel, J. S.; Pflugseder, K.; Gstach, H. *Biotechnol. Bioeng.* **2001**, *7*, 94.

(3) Clapham, B.; Sutherland, A. J. *Tetrahedron Lett.* **2000**, *41*, 2253.

(4) Suresh, S.; Skaria, S.; Ponrathnam, S. *Stud. Surf. Sci. Catal.* **1998**, *113*, 915.

(5) Poornanandhan, A. E.; Rajalingam, P.; Radhakrishnan, G. *Polymer* **1993**, *34*, 1485.

(6) Eder, K.; Buchmeiser, M. R.; Bonn, G. K. *J. Chromatogr., A* **1998**, *810*, 43.

(7) Letourneur, D.; Migonney, V.; Muller, D.; Jozefowicz, M. *J. Chromatogr.* **1992**, *589*, 87.

(8) Gaillard, C.; Camps, M.; Proust, J. P.; Hashieh, I. A.; Rolland, P.; Bois, A. *Polymer* **1999**, *41*, 595.

(9) Viklund, C.; Nordstroem, A.; Irgum, K.; Svec, F.; Frechet, J. M. *Macromolecules* **2001**, *34*, 4361.

(10) Koontz, S. L.; Devivar, R. V.; Peltier, W. J.; Pearson, J. E.; Guillory, T. A. *Colloid Polym. Sci.* **1999**, *277*, 557.

(11) Denes, F. *Trends Polym. Sci.* **1997**, *5*, 23.

(12) Godfrey, S. P.; Kinmond, E. J.; Badyal, J. P. S.; Little, I. R. *Chem. Mater.* **2001**, *13*, 513.

(13) Devivar, R. V.; Koontz, S. L.; Peltier, W. J.; Pearson, J. E.; Guillory, T. A.; Fabricant, J. D. *Bioorg. Med. Chem. Lett.* **1999**, *9*, 1239.

(14) Barrett, E. P.; Joyner, L. G.; Halenda, P. H. *J. Am. Chem. Soc.* **1951**, *73*, 373.

(15) Sing, K. *Colloids Surf., A* **2001**, *187*, 3.

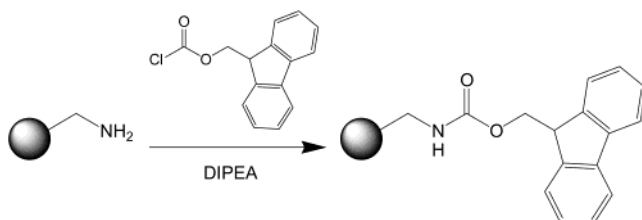
(16) Brunauer, S.; Emmett, P. H.; Teller, E. *J. Am. Chem. Soc.* **1938**, *60*, 309.

Table 1. BET Surface Area and BJH Pore Volume Prior to and Following Allylamine Plasmachemical Functionalization^a

polymer	abbreviation	before plasma treatment		after plasma treatment	
		BET surface area (m ² /g)	BJH pore volume (mL/g)	BET surface area (m ² /g)	BJH pore volume (mL/g)
ArgoPore	AP(154)	626	1.24	529	1.21
PM3-0001	PM(75)	720	1.72	461	1.54
Amberchrom CG-1000	AC(35)	131	0.56	79	0.42
DynoSpheres PD-30	DS(30)	438	2.40	212	0.84
DynoSpheres PD-15	DS(15)	536	1.82	158	0.71

^a The number in brackets for the abbreviation corresponds to the particle size in micrometers.

Scheme 1. Derivatization of Amine Groups on Plasmachemical-Functionalized Polymer Beads with 9-Fluorenylmethyl Chloroformate (Fmoc-Cl)



pump (Edwards E2M2 Fomblin) through a liquid nitrogen cold trap (base pressure below 2×10^{-2} mbar and a leak rate less than 1×10^{-3} mbar min⁻¹). A 13.56 MHz radio frequency (rf) excitation field (ACG-3 ENI generator) was applied via an L-C matching network to a copper coil wound around the glass chamber. Prior to each plasma treatment, the reactor was cleaned with detergent, washed with water, rinsed in propan-2-ol, and then dried. Further cleaning entailed air plasma treatment at 0.2 mbar pressure and 50 W power for 30 min. At this stage, 250 mg of polymer bead material was loaded into the chamber and the system was evacuated. Next, allylamine monomer vapor was introduced at 0.4 mbar pressure, and the electrical discharge was ignited at 20 W power for 20 min. These parameters had previously been optimized on the basis of a 2⁵⁻² reduced factorial design (power, pressure, time, rotation speed, and quantity), followed by Simplex optimization.

Quantification of the number of accessible amine groups introduced by plasmachemical functionalization was achieved by measuring the Fmoc loading.¹⁷ This entailed washing the treated beads in methanol (2×1 mL), and then dichloromethane (2×1 mL) in order to remove any loosely bound material. Subsequent washing in a 20% piperidine/*N,N*-dimethylformamide solution (2×1 mL) dislodged any carbon dioxide adsorbed onto the amine groups. Next, the samples were dried under nitrogen gas, and 20 mg of material was weighed into fritted tubes. In parallel, 10 equiv of 9-fluorenylmethyl chloroformate (Fmoc-Cl) was weighed out into a separate glass vial, dissolved in dichloromethane, and mixed with diisopropylethylamine. A 0.5-mL portion of this solution was aliquoted into each reaction tube. These tubes were then placed onto an orbital shaker (Vibrax VXR) for 30 min, allowing the Fmoc-Cl coupling reaction to proceed to completion. Excess solvent was removed by pumping on a vacuum block, and the remaining material was successively washed in tetrahydrofuran, water, methanol, and dichloromethane (6×1 mL for each solvent). Finally, the samples were dried in a nitrogen atmosphere.

Deprotection of the Fmoc-amine groups involved weighing 10 mg of each dried polymer bead sample into individual 5 mL volumetric flasks, followed by the addition of 1 mL of a 20% piperidine/*N,N*-dimethylformamide solution, and allowing the samples to stand for 30 min. Each solution was diluted with methanol to make a total of 5 mL, and the absorbance at 301 nm associated with the piperidine adduct deprotection product was measured using a UV/vis spectrometer (Uvicam) in conjunction with a reference solution consisting of 1 part 20% piperidine/*N,N*-dimethylformamide to 4 parts methanol. The Fmoc loading for each sample was calculated using the Beer-Lambert law.

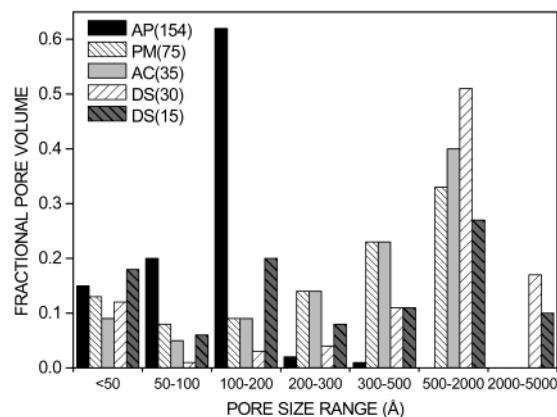


Figure 1. Pore size distribution of porous polymer beads (see Table 1 for key).

The total amount of nitrogen incorporation for the plasma-functionalized polymer spheres (i.e., all types of nitrogen environment) was quantified by elemental CHN analysis (Exeter Analytical Inc. CE 440 elemental analyzer).

To prepare cross sections of polystyrene beads for SEM analysis and Raman mapping, a thin layer of thermoplastic adhesive (Tempfix, Agar Scientific) was melted onto an aluminum plate (1×1 cm), and polymer beads were sprinkled on top. Cooling to room temperature caused the polymer beads to become immobilized on the adhesive surface. This substrate was then mounted onto a cryogenic microtome (Leica RM 2165), and thin slices were cut off the top of the exposed polymer beads to reveal the cross sections. Throughout, the temperature of the substrate holder and knife was kept at -20 °C, while the chamber temperature was maintained at -90 °C.

In the case of SEM analysis, the samples were sputter gold coated and then characterized using a scanning electron microscope (Hitachi S2400 SEM). For chemical quantification, a sample of the cross-sectioned plasma-functionalized polystyrene beads was reacted in a solution containing 4-cyanobenzoic acid (5 equiv) and 1,3-diisopropylcarbodiimide (5 equiv) dissolved in dioxane (1 mL). The resulting cyano Raman band (2220 cm⁻¹) was mapped over the cross-sectioned bead using a Raman microscope system (LABRAM, Jobin Yvon Ltd.). This entailed focusing a laser beam (He-Ne 632.8 nm line, operating at 20 mW) onto the sample surface through the microscope objective and collecting the corresponding Raman signal in a back-scattering configuration with a cooled CCD detector system. The 1800 groove diffraction grating had been calibrated against the reference Si-Si stretching band (521 cm⁻¹) obtained with a silicon wafer. For 2-D chemical mapping, the sample was mounted on a computerized X-Y translational stage and the surface was scanned (1830 – 2630 cm⁻¹) at 1.0-micron intervals. The integrated cyano band (2210 – 2260 cm⁻¹) intensity at each point contributed to the overall surface chemical map.

3. Results and Discussion

The different types of porous polystyrene beads employed in this study were characterized by N₂ sorption analysis, Figure 1 and Table 1. It was found that the ArgoPore (AP) material contains predominantly small

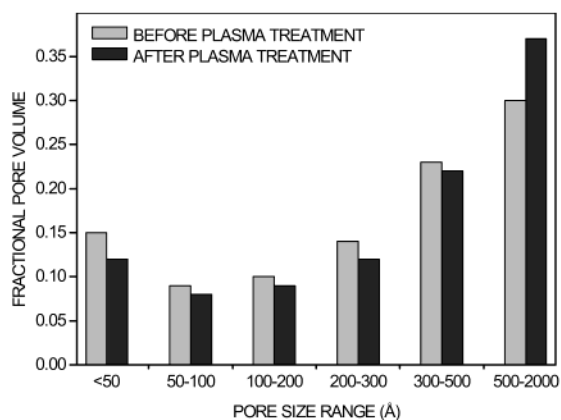


Figure 2. Pore size distribution of PM(75) before and after allylamine plasmachemical modification.

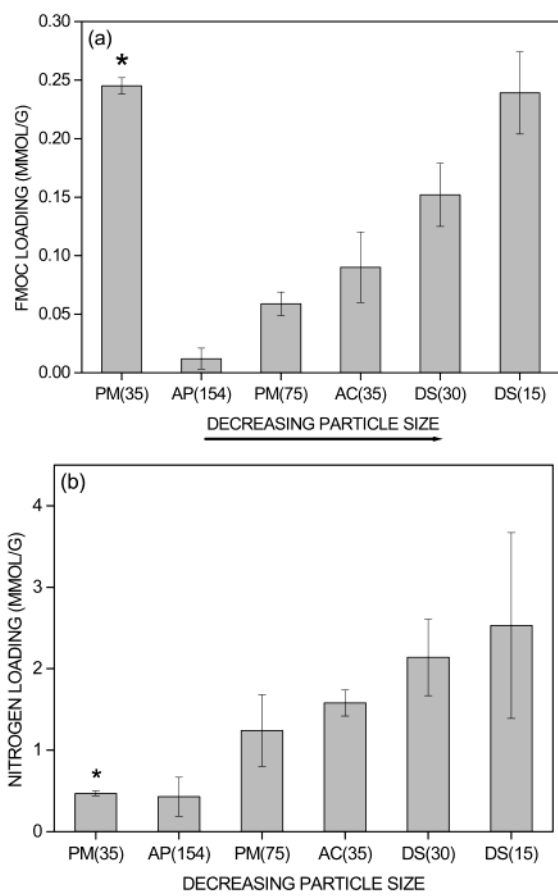


Figure 3. Allylamine plasmachemical functionalization of porous polymer beads: (a) Fmoc loading and (b) nitrogen loading. *Denotes commercial amine-functionalized PM(35) reference material.

pores of less than 200 Å in diameter, while the Dyno-Spheres (DS) had the greatest proportion of large pores (up to 5000 Å in diameter). Amberchrom CG-1000 (AC) and Biosearch PM3-0001 (PM) beads possess intermediate pore size distributions (up to 1000 Å in diameter).

Both the BET surface area and BJH pore volume values decreased upon plasmachemical modification, Table 1. This was accompanied by a shift in the fractional pore volume distribution, Figure 2. The fraction of pores with diameter up to 500 Å decreases (with the most pronounced change occurring for pores below 50 Å). Similar trends were observed for all the different types of polymer bead under investigation, thereby confirming that smaller

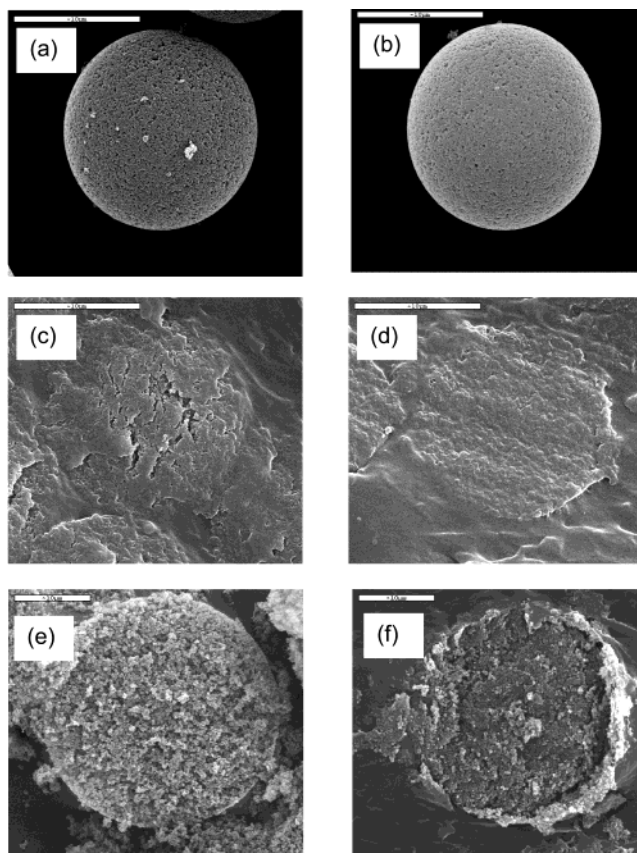


Figure 4. SEM images of (a) untreated whole DS(15), (b) allylamine plasma treated whole DS(15), (c) cross-sectioned untreated DS(15), (d) cross-sectioned allylamine plasma treated DS(15), (e) cross-sectioned untreated DS(30), and (f) cross-sectioned allylamine plasma treated DS(30). Scale bar = 10 μm.

diameter pores undergo preferential filling during plasma-induced polymerization.

Fmoc quantification following allylamine plasmachemical functionalization indicated an inverse correlation to particle size, Figure 3a. A similar trend was noted for nitrogen loading obtained by elemental analysis, Figure 3b. However, the comparatively higher values for the latter indicate that some of the allylamine monomer must undergo fragmentation or rearrangement during plasma activation.¹⁸ Alternatively, there may be amine groups which are inaccessible to the Fmoc-Cl reagent used to determine Fmoc loading (perhaps due to pore blockage). A comparison between approximately similar particle sizes (i.e., AC(35) and DS(30)) illustrates that the presence of larger pores in the DS-type materials is also an important contributing factor. In fact, the Fmoc loading measured for plasma-functionalized DS(15), that is, small particle size with large pores, is found to be comparable to that of commercially available conventional amine-functionalized PM(35) material, Figure 3.

SEM analysis of unmodified DS(15) beads clearly shows a significant number of pore openings at the external surface reflecting the highly porous nature of these materials, Figure 4a. Some dust particles can also be seen. Following allylamine plasma treatment, the surface becomes smoother and the density of pore openings appears to diminish, Figure 4b. Similar trends were observed for the other types of polystyrene bead, thereby

(18) Beck, A. J.; Candan, S.; France, R. M.; Jones, F. R.; Short, R. D. *Plasma Polym.* **1998**, *3*, 97.

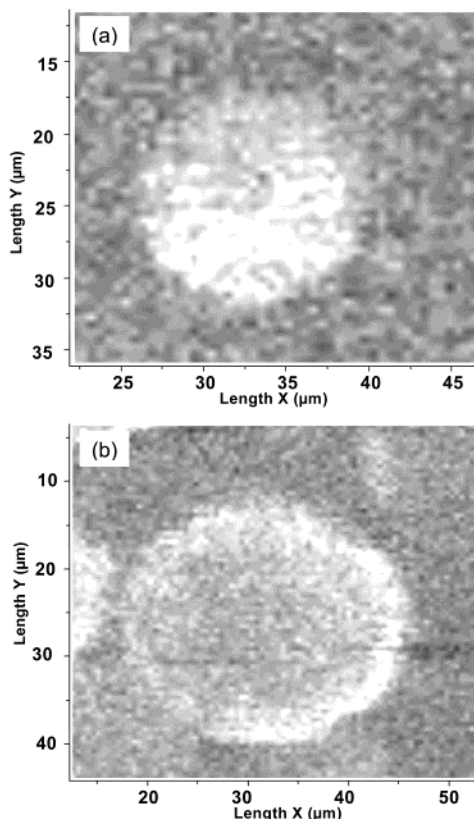


Figure 5. Raman mapping of the CN band (2220 cm^{-1}) following chemical derivatization of cross-sectioned plasma-treated beads: (a) DS(15) and (b) DS(30). (Brightness corresponds to signal intensity.)

confirming that the microsphere exteriors are readily accessible by plasmachemical methods.

The SEM image of a cryogenic cross section of untreated DS(15) indicated that the cutting process leads to very little deformation of the beads (probably attributable to their cross-linked character), Figure 4c. The porous internal structure is clearly discernible. The corresponding cross-sectional SEM image of allylamine plasmachemical functionalized DS(15) shows that the pores have become filled with plasma polymer, Figure 4d. Similarly in the case of DS(30), SEM analysis shows that the plasma species can penetrate inside the beads (smoother appearance), Figure 4e,f. However, the contrast is not as great as previously seen for the DS(15) beads. This difference

can be attributed to the larger spheres experiencing a lower flux of reactive plasma species per unit volume of material due to their inherently smaller effective plasma–solid interfacial area.

Direct visualization of the amine group distribution with depth was achieved by Raman microscopy. This entailed coupling 4-cyanobenzoic acid with amine groups to provide a strong CN Raman signal.¹⁹ Raman mapping of DS(15) beads showed a uniform distribution of amine groups throughout the interior, Figure 5a. This is in good agreement with the SEM images described above. However, in the case of cross-sectioned DS(30) beads, there appears to be preferential accumulation of amine functionalities toward the outer edge, Figure 5b. In this case, the effective penetration depth is estimated to be $3\text{--}4\text{ }\mu\text{m}$.

On the basis of these experiments, it is evident that for a fixed plasma environment, the accessibility of the electrical discharge to the internal pores of a polymer bead is governed by the plasma flux (i.e., inverse correlation to particle size) and diffusion (i.e., the requirement for larger pores). By careful choice of the polymer bead pore architecture, it is possible to functionalize either throughout the bulk or just at the outer surface. The former is better suited for maximizing solid-phase organic synthesis yields, while the latter is more appropriate for reactions with large biomolecules, for example, enzymes or oligonucleotides.²⁰

4. Conclusions

The physical properties of porous polystyrene beads strongly influence their ability to undergo plasmachemical functionalization. In the case of the allylamine precursor, an inverse correlation is found to exist between Fmoc-accessible amine groups and the polymer bead size. This trend can be attributed to the effective plasma–solid interfacial area. Another important factor is pore size, where plasma species are found to penetrate deeper into the interior of polymer spheres containing more open pore architectures.

Acknowledgment. GlaxoSmithKline and EPSRC are thanked for financial support (GR/M95998).

LA0202935

(19) Kress, J.; Rose, A.; Frey, J. G.; Brocklesby, W. S.; Ladlow, M.; Mellor, G. W.; Bradley, M.; *Chem.–Eur. J.* **2001**, *7*, 3880.

(20) Vágner, J.; Barany, G.; Lam, K. S.; Krchnak, V.; Sepetov, N. F.; Ostrem, J. A.; Strop, P.; Lebl, M. *Proc. Natl. Acad. Sci. U.S.A.* **1996**, *93*, 8194.